Synthesis of nanocrystaline CdS thin films by advanced spray pyrolysis technique at low substrate temperature and their characterization

M.D.Uplane*, P.S.Shewale, S.N.Patil
Thin Film Physics Laboratory, Department of Electronics, Shivaji University, Kolhapur-416 004, (INDIA)
E-mail : prashantshewale11@gmail.com

ABSTRACT

Thin films of cadmium sulphide were prepared by advanced spray pyrolysis technique onto glass substrates by spraying aqueous solutions of cadmium chloride and thiourea. The films deposited onto the glass substrates have found to be uniform and well adherent to the substrate. X-ray diffraction analysis revealed that films grown by the new technique are polycrystalline without any second phases; with preferential orientation along the (002), (101) and (200) planes and an average crystallite size of 33.5713 nm. Atomic Force Microscopy pictures showed that substrates were well covered by deposit. The electrical resistivity is approximately 1 Ω-cm. The optical absorption measurement exhibits direct transition with band gap energy of 2.52 eV. The thermoelectric power measurement indicated n-type behavior of cadmium sulphide thin films.   © 2011 Trade Science Inc. - INDIA

INTRODUCTION

Cadmium sulfide (CdS) is a wide bandgap (2.42eV at 300K) compound semiconductor, has emerged as an important material due to its potential applications in optoelectronic devices[1], thin film field effect transistors[2], photo sensors[3] and gas sensors[4]. Over the years, cadmium sulfide thin films have been prepared by many physical and chemical methods, such as vacuum evaporation[5], RF sputtering[6], chemical vapour deposition (CVD)[7], chemical bath deposition (CBD)[8], successive ionic layer adsorption and reaction (SILAR)[9], spray pyrolysis[10], molecular beam epitaxy (MBE)[11] and electrodeposition[12,13]. Among these physical and chemical methods, spray pyrolysis is the simple and low cost technique. Most of the CdS thin films deposited with conventional spray pyrolysis exhibits grain size of the order of micron and high substrate temperature is required to deposit the compound semiconductor. However, there were a few efforts in past to modify conventional spray pyrolysis with respect to its most significant preparative parameter namely the substrate temperature. Some researchers have evaporated CdS thin films at low substrate temperatures[14-16]. Although, A. Ashour has sprayed CdS films at 473K, films are of least quality crystallinity[17]. Most recently, K. Ravichandran et al have employed a simplified spray to fabricate CdS thin films at 543K[18].

In the present investigation an attempt has been made to operate novel advanced two stage spray pyrolysis

Full Paper

technique to demonstrate the successful deposition of the cadmium sulphide films into glasses at low substrate temperature. The structural, electrical and optical properties of the films were studied and results are discussed at length.

EXPERIMENTAL

Figure 1 shows the cross-sectional view of the Advanced Two Stage Spray Pyrolysis System (ATS-SPS). It consists of reaction chamber, substrate heater, temperature controller and nozzle assembly. The nozzle is mounted on the wooden block, which is fixed. The cylindrical furnace is located on MS stand, whereas the substrate heater is resided at the top of cylindrical furnace. The reaction temperature and substrate temperature were controlled by PID temperature controller with ± 3K accuracy. Appropriate exhaust and other required facilities were provided to control the additional parameters precisely.

The details of the mechanism of the advanced spray pyrolysis technique have given elsewhere.

Before deposition, the glass substrates were ultrasonically cleaned in acetone solution, and then rinsed in double distilled water. These cleaned glass substrates were fitted to the surface of substrate heater. The 0.1M and 0.05M aqueous spraying solutions comprised of equimolar concentrations of cadmium chloride and thiourea respectively. The atomization of resulting chemical solution into a spray of fine droplets was achieved by the spray nozzle, with the help of compressed air as carrier gas to obtain CdS thin films at 473K substrate temperature. While deposition, the reaction chamber kept at 573K. The spray rate of 10 ml/min and nozzle-substrate separation of 34cm was maintained constant in order to get uniform and good quality films.

Structural characterization of CdS thin films was carried out by X-ray diffraction (XRD) and atomic force microscopy (AFM). A Phillips PW-1710, grazing angle X-ray diffractometer was used to analyze the crystallinity of CdS films using a Cu-Kα radiation source of wavelength (λ) 0.1540 nm. The surface morphology of the resulting films was investigated using Nanoscope (III-A) AFM equipped with Si_3N_4 tips of 4 nm radius. All AFM pictures were obtained in tapping mode. The scan frequency was in the range of 0.5 s^{-1}. The optical

absorbance of the samples was studied using a UV-VIS-NIR spectrophotometer (Hitachi-330) within the wave length range of 350 to 850 nm. The electrical resistivity was measured by two-probe method within the temperature range of 330 to 523K.

RESULTS AND DISCUSSION

Thoroughly mixed solution of basic ingredients was sprayed through the specially designed glass nozzle. When the solution is sprayed, small aerosols of the solution enter the reaction chamber and thermal decomposition of the initial ingredient takes place and fine particles of CdS were formed by the following reaction.

$$CdCl_2 + (NH_2)_2CS + 2H_2O \rightarrow CdS + 2NH_4Cl + CO_2 \quad (1)$$
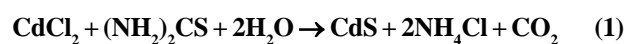
These particles were pushed upward and further collected onto the surface of the glass substrates, which were kept at lower temperature, as compared to the reaction chamber temperature; this yielded a uniform film of CdS onto the glass substrate. Keeping other parameters constant, the thickness of the film was measured as a function of the concentration (M) shown in figure 2. The film thickness is observed to increase with increase in concentration due to the availability of excess cadmium and sulphur atoms in the solution at higher concentration.

The structural characteristics were comprehensively investigated by means of X-ray diffraction (XRD) using Cu-Kα radiation. The XRD pattern of 0.1 M cadmium sulphide thin film prepared at 473K substrate temperature is exposed in figure 3. It exhibits the (100), (002), (101), (103), (200), (112) and (202) peaks corresponding to the hexagonal phase of CdS for all samples under test. It is supplementary distinguished that (002), (101) and (200) diffraction peaks are stronger as compared to the other peaks, which show evidence of strapping orientation along (002), (101) and (200) planes. The results described by Kalafi et al.[13] for escalation of CdS thin films by spray pyrolysis under illumination are analogous with the present work, who excessively have reported predominant orientation in favour of the (101) rather than (002) reflection. The phase identification was done by comparing pragmatic 'd' values with standard JCPDS data and it is established that all the max-outs concur with hexagonal CdS phase. It further reveals that films are liberated

Full Paper

from other impurities and traces of initial ingredients.

The mean crystallite size 'ε' was calculated from full width half-maximum (FWHM) of (101) diffraction peak using Debye-Scherrer formula[19]:

$$\varepsilon = 0.94\ \lambda/\beta\ \cos\theta \qquad (2)$$

where, λ is the X-ray wavelength (1.548 Å for Cu-Kα), θ is diffraction angle and β is the full width half maximum. We have calculated the crystallite size for intense peaks (002), (101) and (200) which are enlisted in TABLE 1 and the average crystallite size obtained is 33.5713 nm. This crystallite size is comparable to that obtained by A. Ashour who has obtained 40nm crystallites by employing conventional spray pyrolysis[17]. So, it is anticipated that our advanced spray pyrolysis technique can be exploited to prepare better nanostructured thin films. The quantity of assorted defects existing in the film was determined by evaluating the dislocation density (δ) using the formula $\delta = \dfrac{1}{D^2}$, where D is the crystallite size[20]. The evaluated dislocation densities are tabulated in TABLE 1.

Further, the information on strain (τ) of the deposited CdS films has been evaluated by the following relation[21]:

$$\frac{\beta \cdot \cos\theta}{\lambda} = \frac{1}{\varepsilon} + \frac{\tau \cdot \sin\theta}{\lambda} \qquad (3)$$

where, τ is average strain, more to the point symbols with their standard implication. Figure 4 demonstrates the variation of $\beta\cos\theta/\lambda$ vs. $\sin\theta/\lambda$ for CdS nanocrystals. The lattice strains are measured for intense peaks (002), (101) and (200), which are specified in TABLE 1 as well. The average strain evaluated is found to be -1.6736×10^{-3}. The lattice strains are negative if the epilayer is beneath compression and it is positive if it is under tension[22]. Accordingly, this estimated value clearly signifies the existing compressive strain.

Figure 5 shows the 2-dimensional atomic force microscopy image of the advanced two stage spray deposited 0.1M CdS film; where small grains of the CdS particles are grouped to form large clusters. Thus various sized grains could be observed on the surface. The average grain size was estimated from higher magnification AFM images. Calculation of grain diameter or grain size is done using Cottrell's method[23]. This method gives the relation between the number of intercepts of the grain boundary per unit length (P), and total number of intercept (n) as,

$$P = \left(\frac{n}{2\pi \cdot r}\right)M \qquad (4)$$

where, 'n', is the number of intersections of grain boundaries with the circle, 'M', is the magnification and 'r', is the radius of circle.

Using 'P', grain diameter ('L') can be calculated as,

$$L = \frac{1}{P-1} \qquad (5)$$

The measurements were carried out on several locations of the film in order to obtain a statistical average value and the grain sizes of the CdS particles are estimated to be approximately in the range of 40-60 nm.

The sample quality was checked through the root mean square roughness parameter (rms) provided by the AFM software. The rms roughness was calculated via the standard formula[24]:

$$\mathrm{rms} = \sqrt{(\Sigma(Z_i\text{-}Z_{avg})^2/N} \qquad (6)$$

It shows the rms surface roughness of a particular image area. This is the standard deviation of the Z value (height value) within the given area. Where Z_{avg} is the average of the Z values within the given area, Z_i is the height value at that point, and N is the number of points within the given area. The 3-dimensional atomic force microscopy image of 0.1 M sample is shown in figure 6. The sample roughness was found to be approximately 22.12 nm. This analytically observed high surface roughness is attributed to the formation of aggregated nanoparticles and not to sprayed droplets reaching directly to substrates.

The electrical resistivity of CdS thin film was studied by two-probe method. The figure 7 describes the variation of log (ρ) with temperature for the present samples. The nature of the plot indicates semiconducting behavior of the material. The room temperature elec-

TABLE 1 : FWHM, Crystallite size, dislocation density and lattice strain along various XRD peaks for 0.1M CdS thin film

XRD Peak	FWHM β ($\times 10^{-3}$ (rad.))	Crystallite size (nm)	Dislocation density(δ) ($\times 10^{14}$ (lines /m^2))	Lattice strain τ ($\times 10^{-3}$)
(002)	4.3227	32.9537	9.2085	-2.0217
(101)	4.6786	30.5622	1.0706	-2.0549
(200)	4.1465	37.1980	7.2270	-0.9441
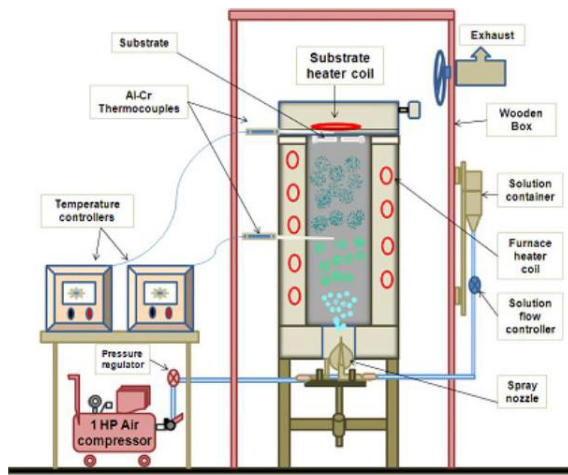
Figure 1 : Cross sectional view of the advanced spray pyrolysis system
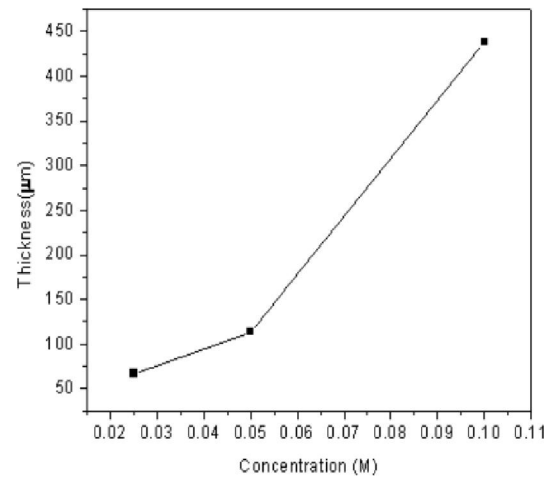
Figure 2 : Thickness (µm) vs. concentration (M)
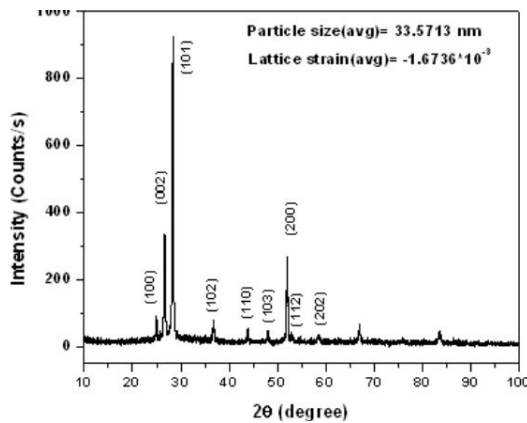
Figure 3 : X-ray diffraction pattern of the sample prepared with 0.1 M concentration

Figure 4 : Bcosθ/λ vs. sinθ/λ for CdS nanocrystals

trical resistivities measured for both (0.05 & 0.1M) samples are of the order of 1.0006863 & 1.00525 Ω-cm respectively. From figure the activation energy (E_a) is calculated by using following resistivity relation[25]:

$$\rho = \rho_o \exp(-E_a/KT) \qquad (7)$$

where E_a is activation energy, ρ is bulk resistivity, K is Boltzmann Constant, T is absolute temperature. The corresponding activation energies are 1.3330×10^{-4} & 1.3604×10^{-4} respectively. The high resistivity values might be due to the scattering of charge carriers at the large number of grain boundaries present in the material[26].

The optical transmission spectra of the CdS films prepared with 0.05M and 0.1M concentration are given in figure 8. The sharp absorption edge is found around 510 nm for both samples. At 550nm, both the samples exhibit transmittance above 87%; which is more supe-

rior to the transmittance obtained by A. Ashour[17] and that obtained by K. Ravichandran et al.[18]. The sharp absorption edge near the band edge exhibits the direct optical transition in CdS.
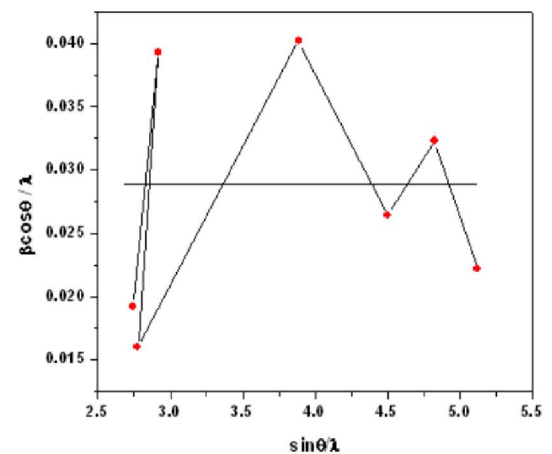
The absorption data was further analyzed by using the following Tauc's expression[27] for near-edge optical absorption of semiconductors:

$$(\alpha h\upsilon) = K(h\upsilon - E_g)^n \qquad (8)$$

where, K is constant, E_g is the separation between the valance and conduction bands, and n is a constant that depends on transition. The n is ½ for direct transition whereas it is 2 for indirect transition, for direct forbidden n=3/2 and for indirect allowed n=3. Since it is well known that the band gap energy largely depends on the particle size, crystal structure and strain in the film; assuming direct transition in CdS material, the direct band gap was determined from the intercept of the straight

Full Paper
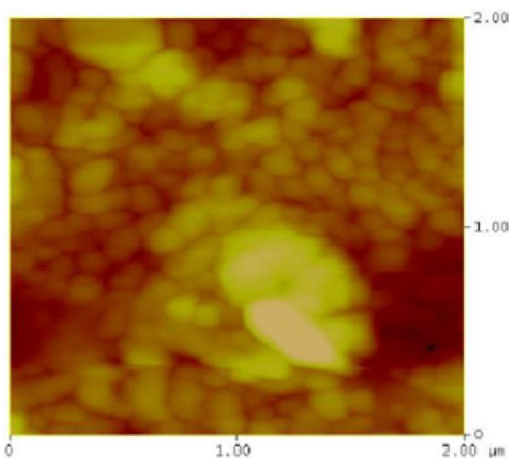
Figure 5 : The 2-dimensional atomic force microscopy image of sample prepared with 0.1 M concentration
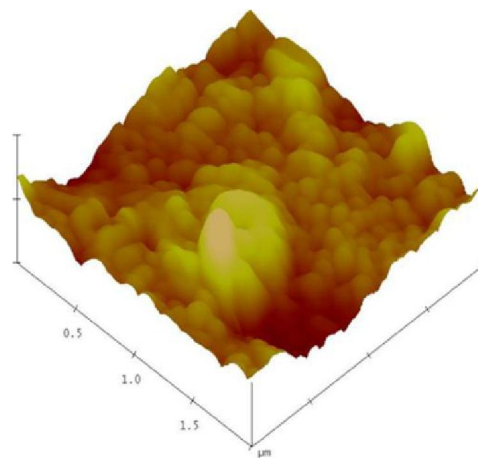
Figure 6: The 3-dimensional atomic force microscopy image of sample prepared with 0.1 M concentration
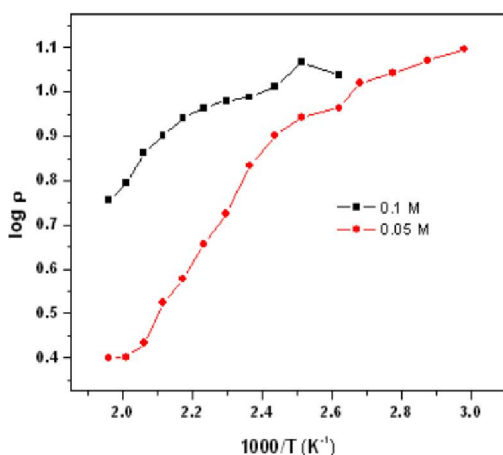
Figure 7 : Variation of the log (ρ) vs. 1000/T
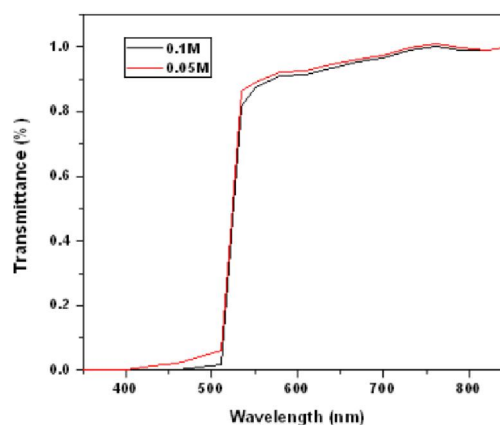
Figure 8 : Variation of transmittance with wavelength of samples prepared with 0.1M and 0.05 M concentrations

portion of the graph of $(ah\upsilon)^2$ versus $h\upsilon$. The band gap value (E_g) calculated from extrapolation of linear fit to the abscissa of this plot is about 2.52 eV. This is slightly higher than, quoted in the literature[28,29]. This may be ascribed to the quantum confinement effect in CdS film[30,31]. Also the increased band gap can be attributed to the existing compressive strain[26].

Moreover considering practically zero absorbance, the refractive index (n) in the visible range between 480 to 800 nm is evaluated by using the formula[33]:

$$n = 1 + R^{1/2} / 1-R^{1/2} \tag{9}$$

Since the transmittance and therefore reflectance possessed by both the samples is nearly overlapping, it is originated that refractive index for given samples remains almost same in the studied wavelength array. Refractive index in such a high transmittance and absorbance range found to be 1.8970. The present refractive index obtained is in good agreement with the earlier reported value[29].

The variation of thermoemf developed across each sample with a change in temperature was measured. Polarity of the themovoltage reveals an n-type semiconducting behavior of CdS. These results are similar to the results reported by others in case of the films prepared by physical and chemical methods.

CONCLUSION

The CdS thin films have been successfully deposited by novel advanced two stage spray pyrolysis method. This anomalous method allowed us to deposit the CdS thin films at relatively low substrate temperature such as 473K. A study has investigated different structural, morphological, electrical and optical assets of CdS deposits. The X-ray diffraction study exposed

the nanocrystalline hexagonal CdS structure comprising lattices underneath the compressive strain. The atomic force spectroscopy revealed the film surface morphology exhibiting small grains of the CdS particles which are grouped to form large clusters. The large grain boundaries caused the scattering of charge carriers which in turn caused high resistivity. The existing strain and quantum confinement effect led the foundation for increase in CdS band gap energy. In short, novel advanced spray pyrolysis could be suitable route for fabrication of many semiconducting compounds.

ACKNOWLEDGEMENT

REFERENCES

[1] X.L.Tong, D.S.Jiang, Z.M.Lim, M.Z.Luo, Y.Li, P.X.Lu, G.Yang, H.Long; Thin Solid Films, **560**, 2003-2008 **(2008)**.

[2] B.Mereu, G.Sarau, E.Pentia, V.Draghici, M.Lisca, T.Botila, L.Pintilie; Mater.Sci.Eng.B, **109**, 260-263 **(2004)**.

[3] R.R.Ahire, N.G.Deshpande, Y.G.Gudage, A.A.Sagade, S.D.Chavhan, D.M.Phaseb, Ramphal Sharma; Actuators A, **140**, 207-214 **(2007)**.

[4] Y.J.Lee, H.B.Kim, Y.R.Roh, H.M.Cho, S.Baik; Actuators A, **5**, 173-178 **(1998)**.

[5] H.Chavez, M.Jordan, J.C.Mcclure, G.Lush, V.P.Singh; J.Mater.Sci.: Mater.Ele., **8**, 151-154 **(1997)**.

[6] Byung-Sik Moon, Jae-Hyeong Lee, Hakkee Jung; Thin Solid Films, **511-512**, 299-303 **(2006)**.

[7] N.I.Fainer, M.L.Kosinova, Y.M.Rumyantsev, E.G.Salman, F.A.Kuznetsov; Thin Solid Films, **280**, 16-19 **(1996)**.

[8] Xiangdong Zhou, Ziheng Li, Zhiyou Li, Shuang Xu; Chem.China., **3**, 18-22 **(2008)**.

[9] A.Ates, M.A.Yildirim, M.Kundakci, M.Yildirim; Chin.J.Phys., **45**, 2-I **(2007)**.

[10] P.Raji, C.Sanjeeviraja, K.Ramachanrdran; Bull.Mater.Sci., **28**, 233-238 **(2005)**.

[11] J.W.Choi, A.Bhupathiraju, M.A.Hasan, J.M.Lannon; J.Cryst.Growth, **255**, 1-7 **(2003)**.

[12] S.J.Lade, M.D.Uplane, C.D.Lokhande; Mater. Chem.Phys., **53**, 239-242 **(1998)**.

[13] M.Kalafi, H.Bidadi, S.Sobhaian, A.I.Bayramov, V.M.Salmanov; Thin Solid Films, **265**, 119-122 **(1995)**.

[14] A.Ashour, R.D.Gould, A.A.Ramadan; Phys. Stat.Sol., **125**, 541-552 **(1991)**.

[15] A.A.Ramadan, R.D.Gould, A.Ashour; Int.J.Electronics, **73**, 717-727 **(1992)**.

[16] A.Ashour, N.El-Kadry, S.A.Mahmoud; Vacuum, **46**, 1419-1421 **(1995)**.

[17] A.Ashour; Turk J.Phys., **27**, 551-558 **(2003)**.

[18] K.Ravichandran, P.Philominathan; App.Surf.Sci., **255**, 5736-5741 **(2009)**.

[19] K.Ravichandran, P.Philominathan; Investigations Sol.Energy, **82**, 1062-1066 **(2008)**.

[20] S.Ilican, Y.Caglar, M.Caglar; J.Optoelectro. Adv.Mater., **10**, 2578-2583 **(2008)**.

[21] P.K.Ghosh, S.Das, K.K.Chattopadhyay; J.Nanoparticle Research, **7**, 219-225 **(2005)**.

[22] S.I.Cho, K.Chang, M.S.Kwon; J.Mater.Sci., **42**, 3569-3572 **(2007)**.

[23] M.G.Chourashiya, J.Y.Patil, S.H.Pawar, L.D.Jadhav; Mater.Chem.Phys., **109**, 39-44 **(2008)**.

[24] M.Suchea, S.Christoulakis, K.Moschovis, N.Katsarakis, G.Kiriakidis; Thin Solid Films, **515**, 551-554 **(2006)**.

[25] J.Jeorge, M.K.Radhakrishnan; Solid State Commun., **33**, 987-989 **(1980)**.

[26] L.C.S.Murthy, K.S.R.K.Rao; Bull.Mater.Sci., **22**, 953-957 **(1999)**.

[27] J.Tauc (Ed.); 'Amorphous and Liquid Semiconductor', Plenum, New York, 159 **(1974)**.

[28] S.M.Sze; 'Physics of Semiconductor Devices', New York, Wiley, 849 **(1981)**.

[29] S.Mahanti, D.Basak, F.Rueda, M.Leon; J.Electron. Mater., **28**, 559-562 **(1999)**.

[30] R.Banerjee, R.Jayakrishnan, P.Ayyub; J.Phys. Condens.Matter., **12**, 10647-10654 **(2000)**.

[31] R.Maity, K.K.Chattopadhyay; J.Nanoparticle Research, **8**, 125-130 **(2006)**.

[32] X.H.Wang, B.Yao, D.Z.Shen, Z.Z.Zhang, B.H.Li, Z.P.Wei, Y.M.Lu, D.X.Zhao, J.Y.Zhang, X.W.Fan, L.X.Guan, C.X.Cong; Solid State Commu., **141**, 600-604 **(2007)**.

[33] B.J.Lokhande, P.S.Patil, M.D.Uplane; Phys.B, **302-303**, 59-63 **(2001)**.